MOLECULAR AND CELLULAR BIOLOGY, Nov. 2006, p. 8042–8051 Vol. 26, No. 21
0270-7306/06/$08.00+0 doi:10.1128/MCB.00722-06

Life with a Single Isoform of Akt: Mice Lacking Akt2 and Akt3 Are Viable but Display Impaired Glucose Homeostasis and Growth Deficiencies▽†

Bettina Dummler,[1] Oliver Tschopp,[1] Debby Hynx,[1] Zhong-Zhou Yang,[1] Stephan Dirnhofer,[2] and Brian A. Hemmings[1]*

Friedrich Miescher Institute for Biomedical Research, Maulbeerstrasse 66, Basel CH-4058, Switzerland,[1] and Institute of Pathology, University of Basel, Schönbeinstrasse 40, Basel CH-4031, Switzerland[2]

Received 26 April 2006/Returned for modification 1 June 2006/Accepted 13 August 2006

To address the issues of isoform redundancy and isoform specificity of the Akt family of protein kinases in vivo, we generated mice deficient in both Akt2 and Akt3. In these mice, only the Akt1 isoform remains to perform essential Akt functions, such as glucose homeostasis, proliferation, differentiation, and early development. Surprisingly, we found that *Akt2*$^{-/-}$ *Akt3*$^{-/-}$ and even *Akt1*$^{+/-}$ *Akt2*$^{-/-}$ *Akt3*$^{-/-}$ mice developed normally and survived with minimal dysfunctions, despite a dramatic reduction of total Akt levels in all tissues. A single functional allele of Akt1 appears to be sufficient for successful embryonic development and postnatal survival. This is in sharp contrast to the previously described lethal phenotypes of *Akt1*$^{-/-}$ *Akt2*$^{-/-}$ mice and *Akt1*$^{-/-}$ *Akt3*$^{-/-}$ mice. However, *Akt2*$^{-/-}$ *Akt3*$^{-/-}$ mice were glucose and insulin intolerant and exhibited an ~25% reduction in body weight compared to wild-type mice. In addition, we found substantial reductions in relative size and weight of the brain and testis in *Akt2*$^{-/-}$ *Akt3*$^{-/-}$ mice, demonstrating an in vivo role for both Akt2 and Akt3 in the determination of whole animal size and individual organ sizes.

The coordination between signal specificity and kinome redundancy is a fundamental issue in cell biology that is not yet fully understood. Although most of the major kinase families are conserved among metazoans, the vertebrate genome contains distinctly more genes encoding protein kinases than do those of worms or flies (24). Duplications of gene loci in vertebrates have led to the expansion of individual kinases into several homologous isoforms and brought about a concomitant increase in signaling complexity. It has been proposed that such isoforms are uniquely adapted to transmit distinct biological signals.

The Akt protein signaling kinase (also known as protein kinase B [PKB]) has a high level of evolutionary conservation and plays a key role in the conserved phosphoinositide 3-kinase (PI3K) signaling pathway (27). In mammals, Akt is implicated in the regulation of widely divergent cellular processes, such as metabolism, differentiation, proliferation, and apoptosis (3, 20). Accordingly, activation of Akt is promoted by numerous stimuli, including growth factors, hormones, and cytokines. There are three isoforms of Akt in mammals, termed Akt1/PKBα, Akt2/PKBβ, and Akt3/PKBγ. These isoforms are products of distinct genes but are highly related, exhibiting >80% protein sequence identity and sharing the same structural organization. To understand the specific physiological functions of the individual isoforms, animal models deficient in Akt1, Akt2, or Akt3 have been generated. Mice lacking Akt1 demonstrate increased perinatal mortality and reductions in body weight of 20 to 30% (6, 8, 38). In contrast, Akt2-deficient mice are born in the expected Mendelian ratio and display normal growth, but they exhibit a diabetes-like syndrome with an elevated fasting plasma glucose level, elevated hepatic glucose output, and peripheral insulin resistance (7, 15). Akt3-deficient mice exhibit a reduction in brain weight resulting from decreases in both cell size and cell number but maintain normal glucose homeostasis and body weights (13, 33). These observations indicate that the three Akt isoforms have some differential, nonredundant physiological functions. The relatively subtle phenotypes of mice lacking individual Akt isoforms as well as the viability of the animals suggest, however, that for many functions Akt isoforms are able to compensate for each other. To address the issue of isoform redundancy, mice with combined Akt deficiencies have been generated. Mice lacking both Akt1 and Akt2 develop to term but die shortly after birth and display multiple defects. They exhibit a severe growth deficiency (body weights at birth are ~50% of normal weights), skeletal muscle atrophy, impaired skin development, and a delay in ossification (25). Mice mutant in both Akt1 and Akt3 die around embryonic day 12, with severe impairments in growth, cardiovascular development, and organization of the nervous system (37). Such data obtained from double knockout mice argue strongly for partially overlapping functions of Akt isoforms in vivo. Certain physiological functions of Akt are thus revealed only when total Akt levels are below a critical threshold in particular cell types and tissues. Here we report the generation of *Akt2*$^{-/-}$ *Akt3*$^{-/-}$ mice to determine the combined roles of these isoforms in Akt-related physiological processes, such as glucose metabolism, development, and growth. It was surprising to us that compound *Akt2*$^{-/-}$ *Akt3*$^{-/-}$ mice and even mice retaining only

* Corresponding author. Mailing address: Friedrich Miescher Institute for Biomedical Research, Maulbeerstrasse 66, Basel CH-4058, Switzerland. Phone: 41 61 697 4872. Fax: 41 61 697 3976. E-mail: brian.hemmings@fmi.ch.

† Supplemental material for this article may be found at http://mcb.asm.org/.

▽ Published ahead of print on 21 August 2006.

one functional allele of Akt1 (*Akt1*$^{+/-}$ *Akt2*$^{-/-}$ *Akt3*$^{-/-}$) were viable and did not display any gross abnormalities. The body size of *Akt2*$^{-/-}$ *Akt3*$^{-/-}$ mice was reduced at birth and throughout postnatal life, and they exhibited severe glucose and insulin intolerance.

MATERIALS AND METHODS

Mice. Akt3 mutant mice were generated as described previously (33). For the generation of Akt2 mutant mice, an ~9.4-kb mouse genomic DNA fragment containing exons 3 and 4 of the *Akt2* gene was subcloned into pBluescript, and a NotI site was generated in exon 4 by PCR. An ~5-kb IRES-*lacZ*-Neo^r cassette was inserted into the NotI site, resulting in partial deletion of exon 4 and a frameshift in the open reading frame of the *Akt2* gene. The resulting targeting vector was linearized with SalI and electroporated into 129/Ola embryonic stem (ES) cells. Screening of ES cell clones was performed by Southern blotting. DNAs were digested with EcoRI and probed with an external probe (see Fig. S2a, probe A, in the supplemental material). An internal probe (see Fig. S2a, probe B, in the supplemental material) was then used on BamHI-digested DNAs for further characterization of ES cell clones positive for homologous recombination. Correctly targeted ES cells were used to generate chimeras. Male chimeras were mated with wild-type C57BL/6 females to obtain *Akt2*$^{+/-}$ mice, which were intercrossed to produce Akt2 homozygous mutants. Progeny were genotyped for the presence of a targeted *Akt2* allele by multiplex PCR. The following primers were used for genotyping: P1-as, 5′-CTCAGGGACACCCAT GTGTGGCTGC-3′; P2/KO-s, 5′-GCTGCCTCGTCCTGCAGTTCATTC-3′; and P3/WT-s, 5′-CCACAGGCAGCAGAAAGGAA-3′. One primer set amplifies a 600-bp fragment from the targeted allele, and the second primer set amplifies a 360-bp fragment from the wild-type allele. *Akt2*$^{-/-}$ *Akt3*$^{+/+}$ mice were crossed with *Akt2*$^{+/+}$*Akt3*$^{-/-}$ mice to obtain *Akt2*$^{+/-}$ *Akt3*$^{+/-}$ offspring, which were mated to generate *Akt2*$^{-/-}$ *Akt3*$^{-/-}$ mice as well as the wild-type, *Akt2*$^{-/-}$, and *Akt3*$^{-/-}$ littermates used in the study. Both starting strains were on a mixed 129 Ola and C57BL/6 background. For the generation of *Akt1*$^{+/-}$ *Akt2*$^{-/-}$ *Akt3*$^{-/-}$ mice, *Akt2*$^{-/-}$ *Akt3*$^{-/-}$ mice were mated with *Akt1*$^{+/-}$ *Akt3*$^{-/-}$ mice (37), and resulting *Akt1*$^{+/-}$ *Akt2*$^{+/-}$ *Akt3*$^{-/-}$ progeny were intercrossed. Mice were housed according to the Swiss Animal Protection Laws in groups with 12-h dark-light cycles and with free access to food and water. All procedures were conducted with the relevant approval of the appropriate authorities.

Cell culture. Cerebellar granule cells were isolated and cultured as previously described (28). Cells were counted and plated on poly-D-lysine-coated six-well plates in culture medium (basal Eagle medium containing 10% fetal bovine serum, 100 U of penicillin-streptomycin, 2 mM glutamine, and 25 mM KCl). After 24 h, 10 μM cytosine arabinoside was added to the medium to inhibit the proliferation of nonneuronal cells. After 2 days in culture, cells were starved by serum deprivation for 12 h and then stimulated with 100 nM insulin.

Western blot analysis. For Western blot analysis, protein lysates were prepared by homogenization of various organs in lysis buffer (50 mM Tris-HCl, pH 8.0, 120 mM NaCl, 1% NP-40, 40 mM β-glycerophosphate, 10% glycerol, 4 μM leupeptin, 0.05 mM phenylmethylsulfonyl fluoride, 1 mM benzamidine, 50 mM NaF, 1 mM Na_3VO_4, 5 mM EDTA, 1 μM Microcystin LR). Homogenates were centrifuged twice (13,000 rpm for 10 min at 4°C) to remove cell debris. Protein concentrations were determined using the Bradford assay. Proteins (50 μg per sample) were separated by 15%, 10%, or 6% sodium dodecyl sulfate-polyacrylamide gel electrophoresis and then transferred to Immobilon-P polyvinylidene difluoride membranes (Millipore). Akt isoform-specific antibodies were obtained by immunizing rabbits with isoform-specific peptides as previously described (38). Antibodies against total Akt, phospho-Akt (Ser473), phospho-glycogen synthase kinase 3α/β (phospho-GSK3α/β [Ser21/9]), phospho-GSK3β (Ser9), total GSK3β, phospho-TSC2 (Thr1462), phospho-p70 S6K (Thr389), and total 4E-BP1 were purchased from Cell Signaling Technologies. Anti-Foxo3a and anti-phospho-Foxo3a (Thr32) antibodies were obtained from Upstate Biotechnology. A rat monoclonal anti-α-tubulin (YL1/2)-producing hybridoma cell line was obtained from the American Type Culture Collection. Anti-TSC2 antibody was generated as previously described (35) and kindly provided by K. Molle (Biozentrum, University of Basel, Switzerland). For quantitation, Western blots were scanned using a GS-800 Bio-Rad densitometer with a resolution of 63.5 μm by 63.5 μm, and bands were quantified using Proteomweaver 4.0.0.5 (Bio-Rad). As shown in Fig. S1 in the supplemental material, the anti-total Akt and anti-phospho-Akt (Ser473) antibodies utilized in this study show equal affinities towards Akt1 and Akt3 but a lower affinity towards Akt2. As a consequence, the total Akt and phospho-Akt levels that were detected in our study with these antibodies may slightly understate the magnitude of the differences between wild-type and *Akt2*$^{-/-}$ *Akt3*$^{-/-}$ mice.

Histology and TUNEL assays. For histological analysis, organs were dissected and fixed in 4% paraformaldehyde–phosphate-buffered saline overnight at 4°C. After dehydration in ethanol, samples were embedded in paraffin. Tissues were cut into 6-μm-thick sections and stored for staining. For hematoxylin-eosin (Sigma) and cresyl violet (Sigma) staining, sections were deparaffinized and stained. A terminal deoxynucleotidyltransferase-mediated dUTP-biotin nick end labeling (TUNEL) assay was performed as previously described (37). For quantitation of apoptosis in testes, sections of testes derived from wild-type and *Akt2*$^{-/-}$ *Akt3*$^{-/-}$ mice were subjected to TUNEL assay, and the number of TUNEL-positive cells per area was counted (for each mouse, an area of ~20 to 40 mm^2 of stained testis sections was analyzed).

Testosterone measurement. Blood samples were collected from tail veins of 10-week-old male mice. Samples were allowed to clot at room temperature, and serum was separated by centrifugation. To account for the pulsatile secretion of testosterone, three separate samples were taken from each mouse on the same day (spaced 3 h apart) and pooled. A commercial enzyme-linked immunosorbent assay kit (DRG Instruments GmbH, Marburg, Germany) was used to measure testosterone in serum following the manufacturer's recommendations.

Glucose and insulin tolerance test. All mice used for glucose and insulin tolerance tests were offspring from doubly heterozygous parents. Note that glucose and insulin tolerance was not affected in doubly heterozygous mice, and an influence of the mother on the diabetic phenotype of the offspring could therefore be excluded. Three-month-old mice of the selected genotypes were made to fast overnight; for glucose tolerance tests, glucose (2 g/kg of body weight) (D-(+)-glucose anhydrous; Fluka) was given orally, and for insulin tolerance tests, insulin (1 U/kg) (human recombinant insulin; Sigma) was administered by intraperitoneal injection. Blood samples were collected at the indicated times from tail veins, and glucose levels were determined using Glucometer Elite (Bayer). Similarly, random-fed and fasting blood glucose levels were determined for 3-month-old mice by the collection of blood samples from tail veins, with glucose levels determined as described above. Blood insulin levels were measured with an ultrasensitive mouse insulin enzyme-linked immunosorbent assay (Immunodiagnostic Systems).

In vivo insulin stimulation. In vivo insulin stimulation was performed on ~8-week-old male mice. Following an overnight fast, a bolus of insulin (1 mU/g or 10 mU/g, as indicated) (human recombinant insulin; Sigma) or saline solution was injected via the inferior vena cava into terminally anesthetized mice. White adipose tissue, liver, skeletal muscle, and whole brain were harvested after 12 min of stimulation and immediately snap frozen in liquid nitrogen. Tissues were homogenized thereafter and lysed as described above.

Statistics. Data are provided as arithmetic means ± standard errors of the means (SEM), and n represents the number of independent experiments. All data were tested for significance using one-way analysis of variance (ANOVA) and a paired or unpaired Student t test, as applicable. Only results with P values of <0.05 were considered statistically significant.

RESULTS

A single functional allele of Akt1 is sufficient for successful embryonic development and postnatal survival in mice lacking Akt2 and Akt3. Considering the lethal phenotypes and multiple developmental defects of *Akt1*$^{-/-}$ *Akt2*$^{-/-}$ and *Akt1*$^{-/-}$ *Akt3*$^{-/-}$ mice, Akt isoforms appear to play essential roles in various aspects of embryonic development (25, 37). Moreover, the *Akt* genes seem to compensate functionally for one another in vivo, as no developmental deficiencies have been observed in any mice lacking only one isoform of the Akt family (6–8, 13, 15, 33). We wanted to evaluate the impact of combined Akt2 and Akt3 deficiencies on the viability and embryonic development of mice. *Akt2*$^{-/-}$ mice were generated by targeted disruption of exon 4 of the *Akt2* gene (see Fig. S2a in the supplemental material). In mice homozygous for the targeted allele, expression of the Akt2 protein was not detectable with isoform-specific antisera (see Fig. S2c in the supplemental material). Thus, the targeted disruption resulted in a functional null allele. *Akt2*$^{-/-}$ *Akt3*$^{+/+}$ mice were crossed with *Akt2*$^{+/+}$

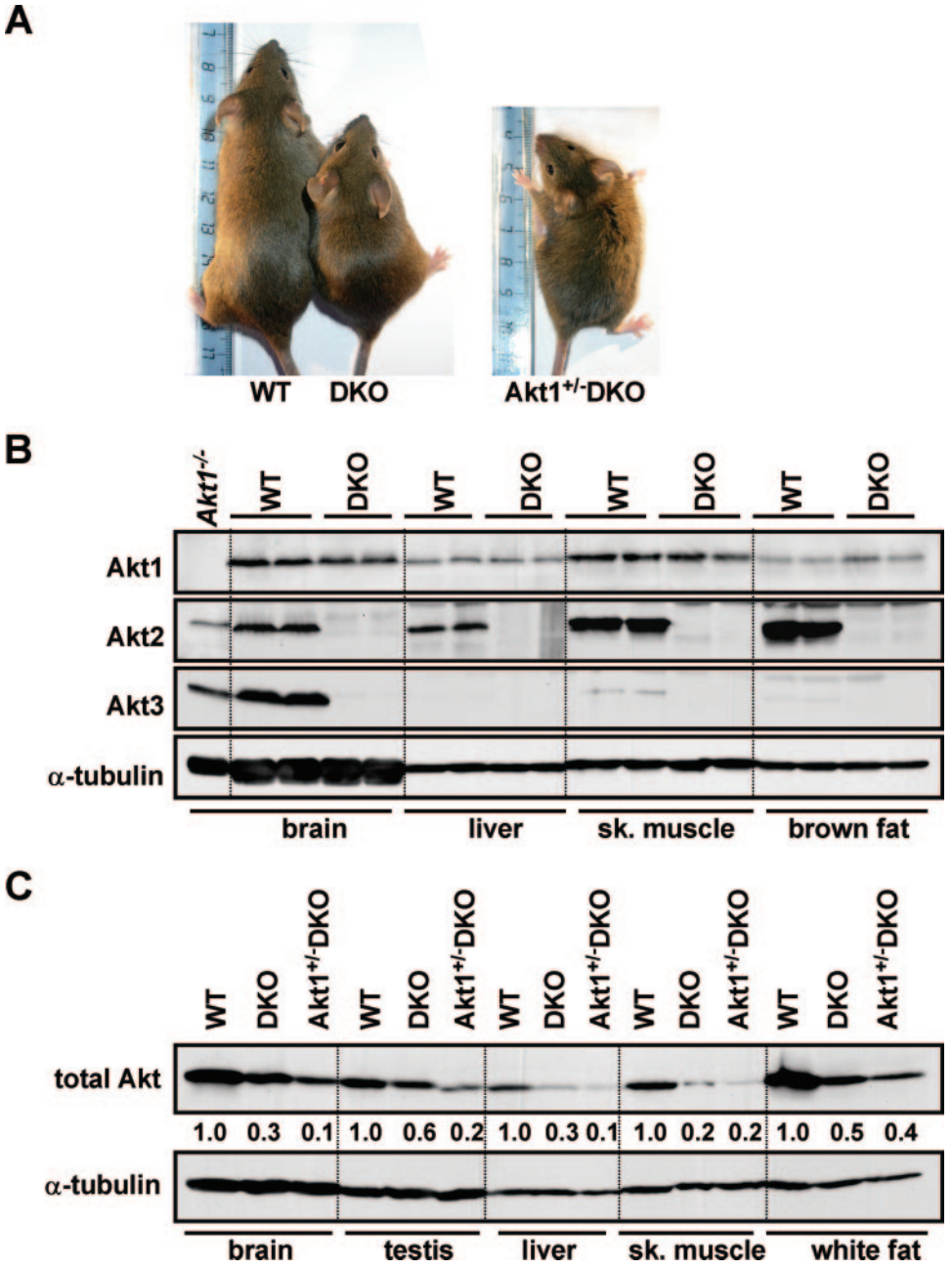

FIG. 1. (A) Top view of wild-type (WT), *Akt2*$^{-/-}$ *Akt3*$^{-/-}$ (DKO), and *Akt1*$^{+/-}$ *Akt2*$^{-/-}$ *Akt3*$^{-/-}$ (Akt1$^{+/-}$DKO) mice (12-week-old male mice; the WT and DKO mice were from the same litter). Note that the pictures are illustrative of the viability of mutant mice rather than a size comparison. (B) Akt1 protein levels in 4-day-old wild-type (WT) and *Akt2*$^{-/-}$ *Akt3*$^{-/-}$ (DKO) pups. The indicated tissues from wild-type and DKO pups were lysed and blotted with antibodies specific for Akt1, Akt2, and Akt3. As a loading control, the expression of α-tubulin was detected on the same membrane. Duplicates are from independent samples. (C) Stepwise reduction of total Akt levels in wild-type (WT), *Akt2*$^{-/-}$ *Akt3*$^{-/-}$ (DKO), and *Akt*$^{+/-}$ *Akt2*$^{-/-}$ *Akt3*$^{-/-}$ (Akt$^{+/-}$DKO) mice. Tissues from 3-month-old mice of the indicated genotypes were lysed and blotted with an Akt antibody that recognizes all three isoforms. As a loading control, the expression of α-tubulin was detected on the same membrane. Bands were quantified, and indicated values represent total Akt expression relative to wild-type expression levels, normalized to the α-tubulin control. The experiment was performed twice with independent samples and with similar results.

Akt3$^{-/-}$ mice to obtain *Akt2*$^{+/-}$ *Akt3*$^{+/-}$ mice. These doubly heterozygous mice were intercrossed to generate *Akt2*$^{-/-}$ *Akt3*$^{-/-}$ mice. Surprisingly, *Akt2*$^{-/-}$ *Akt3*$^{-/-}$ offspring were viable and showed no obvious abnormalities, except for their smaller size (Fig. 1A). Examination of >500 pups from matings between *Akt2*$^{+/-}$ *Akt3*$^{+/-}$ mice showed the expected Mendelian distribution for *Akt2*$^{-/-}$ *Akt3*$^{-/-}$ progeny and the other resulting genotypes (see Table S1 in the supplemental material). We investigated whether upregulation of the remaining Akt isoform in these mice, Akt1, could account for the mild phenotype of *Akt2*$^{-/-}$ *Akt3*$^{-/-}$ mice. Immunoblotting of protein extracts from various tissues of 4-day-old *Akt2*$^{-/-}$ *Akt3*$^{-/-}$

mice with an isoform-specific antibody against Akt1 revealed no significant increase in Akt1 protein levels compared to those in wild-type littermates (Fig. 1B). Since we had previously observed that in neonates the tissue distribution of Akt isoforms differs from that in adult mice (37), we also examined Akt1 expression levels in tissues of adult *Akt2*$^{-/-}$ *Akt3*$^{-/-}$ mice. As in neonates, Akt1 was not upregulated in tissues of adult *Akt2*$^{-/-}$ *Akt3*$^{-/-}$ mice (data not shown). We therefore excluded the possibility that a compensatory upregulation of Akt1 could influence the phenotype of *Akt2*$^{-/-}$ *Akt3*$^{-/-}$ mice.

Next, we asked the question of whether Akt1 affects mouse development in a dose-dependent fashion. To evaluate the impact of a decrease in the Akt1 dose, we crossed our *Akt2*$^{-/-}$ *Akt3*$^{-/-}$ mice with *Akt1*$^{+/-}$ *Akt3*$^{-/-}$ mice (38). Resulting *Akt1*$^{+/-}$ *Akt2*$^{+/-}$ *Akt3*$^{-/-}$ mice were subsequently intercrossed to obtain mice containing only one functional allele of *Akt1* (*Akt1*$^{+/-}$ *Akt2*$^{-/-}$ *Akt3*$^{-/-}$ mice). We did not obtain any *Akt1*$^{-/-}$ *Akt2*$^{-/-}$ *Akt3*$^{-/-}$ mice, as a combined deficiency of Akt1 and Akt3 is lethal at embryonic stage E12 (37). However, we obtained viable *Akt1*$^{+/-}$ *Akt2*$^{-/-}$ *Akt3*$^{-/-}$ mice from these crosses (Fig. 1A; see Table S2 in the supplemental material). Approximately 14% of the mice in the analyzed cohort (n = 105) were *Akt1*$^{+/-}$ *Akt2*$^{-/-}$ *Akt3*$^{-/-}$ mutants. As shown in Fig. 1C, a stepwise reduction in functional *Akt* alleles was reflected by a concomitant reduction in total Akt protein levels. For instance, in both brain and liver, there was an ~3-fold reduction of total Akt levels in *Akt2*$^{-/-}$ *Akt3*$^{-/-}$ mice and an ~10-fold reduction of total Akt levels in *Akt1*$^{+/-}$ *Akt2*$^{-/-}$ *Akt3*$^{-/-}$ mice compared to wild-type levels (Fig. 1C). *Akt1*$^{+/-}$ *Akt2*$^{-/-}$ *Akt3*$^{-/-}$ mice developed normally, with no obvious defects except for a severe growth deficiency, with body weights at the age of 12 weeks reduced ~40% compared to those of wild-type mice (17.1 ± 1.7 g versus 29.1 ± 0.7 g, respectively [n = 5]; $P <$ 0.01). Taken together, these findings demonstrate that Akt1 (even in the case where only one allele is present) is sufficient to enable successful embryonic development and postnatal survival in mice lacking Akt2 and Akt3.

Growth deficiency and substantially reduced brain and testis mass in *Akt2*$^{-/-}$ *Akt3*$^{-/-}$ mice. It was previously shown that disruption of the *Akt1* gene in mice leads to growth retardation (6, 8, 38), and Akt3-deficient mice were shown to have a reduction in brain size (13, 33). In progeny of *Akt2*$^{+/-}$ *Akt3*$^{+/-}$ intercrosses, we observed that the combined deletion of Akt2 and Akt3 resulted in a growth deficiency in both male and female *Akt2*$^{-/-}$ *Akt3*$^{-/-}$ mice. One-week-old male *Akt2*$^{-/-}$ *Akt3*$^{-/-}$ mice were ~28% smaller than their wild-type littermates (3.81 ± 0.21 g versus 5.26 ± 0.14 g; $P < 0.001$), and an average decrease in body weight of 25% persisted throughout the examined 3-month life period of male *Akt2*$^{-/-}$ *Akt3*$^{-/-}$ mice (Fig. 2). For female *Akt2*$^{-/-}$ *Akt3*$^{-/-}$ mice, a significant decrease in body weight was evident only from the fourth week of age onward, with an average decrease of 14% compared to wild-type littermates. Consistent with previous reports, single knockouts of either Akt2 or Akt3 did not significantly affect animal size compared to wild-type littermates (data not shown) (7, 33). Comparisons of selected organ weights (brain, heart, lung, thymus, liver, spleen, kidney, and testis) from 3-month-old *Akt2*$^{-/-}$ *Akt3*$^{-/-}$, *Akt2*$^{-/-}$, *Akt3*$^{-/-}$, and wild-type littermate mice revealed an ~35% reduction in brain weights of

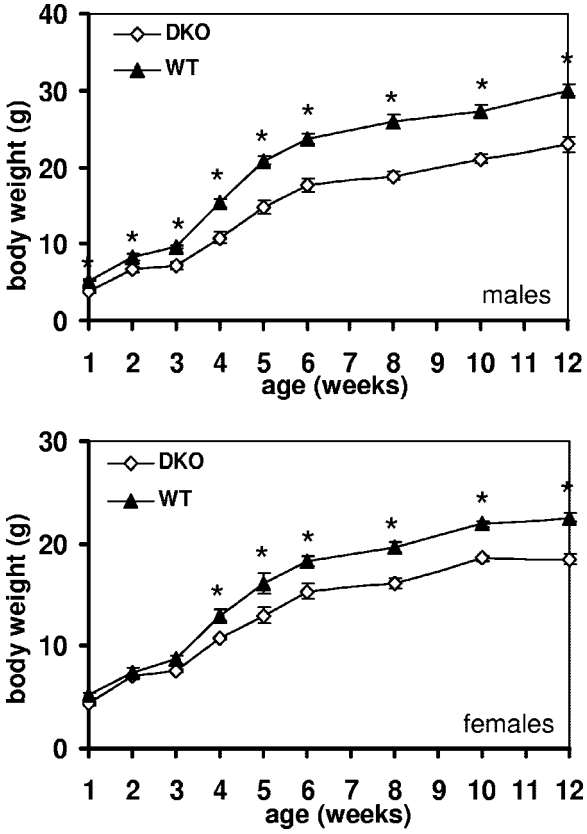

FIG. 2. Growth deficiency in *Akt2*$^{-/-}$ *Akt3*$^{-/-}$ (DKO) mice. Body weights of male (upper panel) and female (lower panel) wild-type (filled triangles) and *Akt2*$^{-/-}$ *Akt3*$^{-/-}$ (open diamonds) littermate mice were determined at the indicated time points. The graph depicts arithmetic means ± SEM (n = 8 for each group). Significantly different values for *Akt2*$^{-/-}$ *Akt3*$^{-/-}$ mice versus the wild type, as determined by one-way ANOVA, are indicated (*, $P < 0.05$).

Akt2$^{-/-}$ *Akt3*$^{-/-}$ mice (0.31 ± 0.01 g versus 0.49 ± 0.01 g; $P <$ 0.001) and an ~40% reduction in testis weights (0.12 ± 0.01 g versus 0.20 ± 0.01 g; $P < 0.001$) compared to those of wild-type mice (Fig. 3A and B). While most organs of *Akt2*$^{-/-}$ *Akt3*$^{-/-}$ mice were decreased proportionally to the reduced body weights, the relative weights of brains and testes were reduced by 18.8% ± 1.7% and 28.5% ± 2.7%, respectively (Fig. 3A and B). The prominent size reduction in the testes prompted us to measure serum testosterone levels in 10-week-old male *Akt2*$^{-/-}$ *Akt3*$^{-/-}$ and wild-type mice. In *Akt2*$^{-/-}$ *Akt3*$^{-/-}$ mice, testosterone levels were ~70% lower than those measured in wild-type mice (1.4 ± 0.5 ng/ml versus 4.7 ± 1.2 ng/ml [n = 5]; $P < 0.05$). In addition, we compared ovary weights in 3-month-old *Akt2*$^{-/-}$ *Akt3*$^{-/-}$ and wild-type females. We observed an ~26% reduction in absolute weights of ovaries of *Akt2*$^{-/-}$ *Akt3*$^{-/-}$ mice (13.3 ± 1.3 mg versus 18.2 ± 1.0 mg [n = 5]; $P <$ 0.05); however, there was no significant difference from the wild type in the organ/body weight ratio.

The PI3K/Akt pathway also plays a critical role in cell survival and apoptosis, and therefore we assessed whether an increased rate of spontaneous apoptosis could account for the smaller sizes of testes in *Akt2*$^{-/-}$ *Akt3*$^{-/-}$ mice. TUNEL assays were performed on testis sections from adult *Akt2*$^{-/-}$ *Akt3*$^{-/-}$

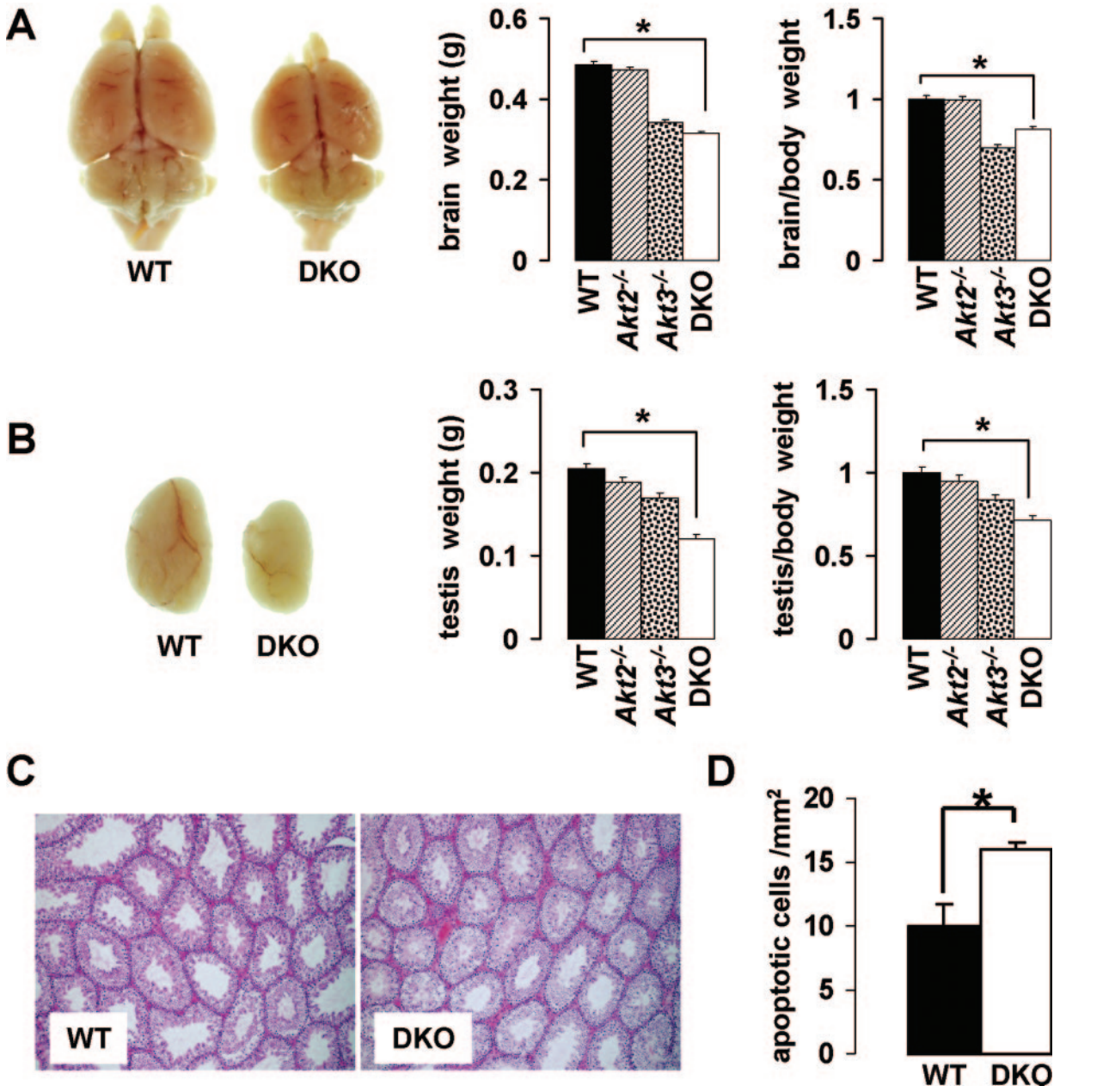

FIG. 3. Selective reduction of brain and testis size in $Akt2^{-/-}$ $Akt3^{-/-}$ mice. (A) Brains were dissected from 3-month-old male wild-type (WT) and $Akt2^{-/-}$ $Akt3^{-/-}$ (DKO) littermate mice (left). Mean absolute brain weights (middle) and brain weights relative to body weight (right) of 3-month-old male mice of the indicated genotypes are shown ($n = 8$; *, $P < 0.001$). (B) Testes were dissected from 3-month-old wild-type and $Akt2^{-/-}$ $Akt3^{-/-}$ littermate mice (left). Mean absolute testis weights (middle) and testis weights relative to body weight (right) of 3-month-old mice of the indicated genotypes are depicted ($n = 14$; *, $P < 0.001$). Relative weights are percentages relative to the wild type (WT = 1). Error bars represent SEM. (C) Morphology of testes from wild-type and $Akt2^{-/-}$ $Akt3^{-/-}$ littermate mice. Representative sections stained with hematoxylin and eosin show morphologically normal seminiferous tubules. (D) Spontaneous apoptosis in testes of $Akt2^{-/-}$ $Akt3^{-/-}$ mice. The graph shows a comparison of TUNEL-positive cell numbers in testis sections from $Akt2^{-/-}$ $Akt3^{-/-}$ mice and their wild-type littermates ($n = 3$; *, $P < 0.05$).

mice and their wild-type littermates. Generally, the rate of spontaneous apoptosis was low for both genotypes, but the testes of $Akt2^{-/-}$ $Akt3^{-/-}$ mice showed an ~1.5-fold increase in TUNEL-positive cells compared to wild-type littermates (Fig. 3D). In addition, areas of seminiferous tubules were reduced ~24% in $Akt2^{-/-}$ $Akt3^{-/-}$ mice compared to those in wild-type littermates (0.76 ± 0.05 versus 1.0 ± 0.05 [$n = 4$]; $P < 0.05$). However, histopathological analysis of testes from $Akt2^{-/-}$ $Akt3^{-/-}$, $Akt2^{-/-}$, $Akt3^{-/-}$, and wild-type littermate mice (3-month-old mice; $n = 5$ to 8 mice per genotype) revealed no morphological abnormalities (Fig. 3C). Furthermore, both male and female $Akt2^{-/-}$ $Akt3^{-/-}$ mice were fertile, although litter sizes from such crossings were smaller (data not shown).

Akt1 is sufficient for phosphorylation of key downstream targets in brains and testes of *Akt2*$^{-/-}$ *Akt3*$^{-/-}$ mice. We were interested to know how Akt signaling was affected in the brains and testes of *Akt2*$^{-/-}$ *Akt3*$^{-/-}$ mice. First, we assessed steady-state phosphorylation/activation levels of Akt in brains and testes of adult *Akt2*$^{-/-}$ *Akt3*$^{-/-}$ and wild-type mice by immunoblotting protein extracts with an antibody against phospho-Ser473. This phosphorylation site is a distinctive indicator of Akt activation status, and the antibody detects phosphorylation of this site in all three Akt isoforms. In the testes of *Akt2*$^{-/-}$ *Akt3*$^{-/-}$ mice, steady-state phosphorylation of Akt was reduced ~10-fold compared to that in wild-type littermate controls and represented residual Akt1 activity (Fig. 4A and B). Interestingly, we found that in vivo insulin stimulation could increase the phosphorylation of Akt in testes of wild-type mice, although this induction was less prominent than that in a classical insulin-responsive tissue, such as the liver, and was scarcely detectable in *Akt2*$^{-/-}$ *Akt3*$^{-/-}$ mice (see Fig. S3 in the supplemental material). Similarly, phosphorylation of Akt in the brain was severely reduced (Fig. 5C shows phospho-Akt under fasting and insulin-stimulated conditions; data for steady state not shown).

Next, we generated primary cultures of cerebellar granule cells to study inducible Akt activation in an in vitro cellular system. In wild-type cerebellar granule cells, the expression of all three Akt isoforms could be detected by isoform-specific antibodies (data not shown), and there was no compensatory upregulation of Akt1 in cells of *Akt2*$^{-/-}$ *Akt3*$^{-/-}$ mice (Fig. 4C). Cerebellar granule cell cultures were deprived of serum for 12 h and then stimulated with 100 nM insulin. After serum deprivation, phospho-Akt levels were >10-fold lower in *Akt2*$^{-/-}$ *Akt3*$^{-/-}$ cells than in wild-type cells, and after stimulation, phospho-Akt levels increased in both wild-type and *Akt2*$^{-/-}$ *Akt3*$^{-/-}$ cells but remained ~2-fold lower in *Akt2*$^{-/-}$ *Akt3*$^{-/-}$ cells (Fig. 4C). We then assessed the phosphorylation levels of several downstream targets of Akt. GSK3 is a key molecule implicated in neuronal survival, protein synthesis, and glycogen synthesis (10–12), whereas tuberous sclerosis complex 2 (TSC2) is a critical target of Akt in mediating cell growth (17, 23, 26) and p70 S6 kinase (S6K) is a downstream component of the PI3K/Akt/TSC pathway (19, 22). Both GSK3 and TSC2 are well-established Akt substrates. In contrast, the regulation of S6K is more complex, as both PI3K-dependent and -independent signaling pathways are involved in its activation (5, 9, 14). Upon insulin stimulation, a clear induction in phosphorylation of all three downstream targets could be observed in cerebellar granule cells, but interestingly, no differences in phosphorylation levels were apparent in *Akt2*$^{-/-}$ *Akt3*$^{-/-}$ cells compared to wild-type cells (Fig. 4C). Similarly, no significant differences in phosphorylation levels of these downstream targets were apparent in the testis (Fig. 4B). We also assessed phosphorylation of the Akt substrate Foxo3a and of the mammalian target of rapamycin (mTOR) substrate 4E-binding protein 1 in testes of *Akt2*$^{-/-}$ *Akt3*$^{-/-}$ mice but found no marked differences compared to the wild type (see Fig. S3 in the supplemental material). In summary, residual Akt1 activity appears be sufficient to phosphorylate these downstream targets under both steady-state and induced conditions in *Akt2*$^{-/-}$ *Akt3*$^{-/-}$ mice.

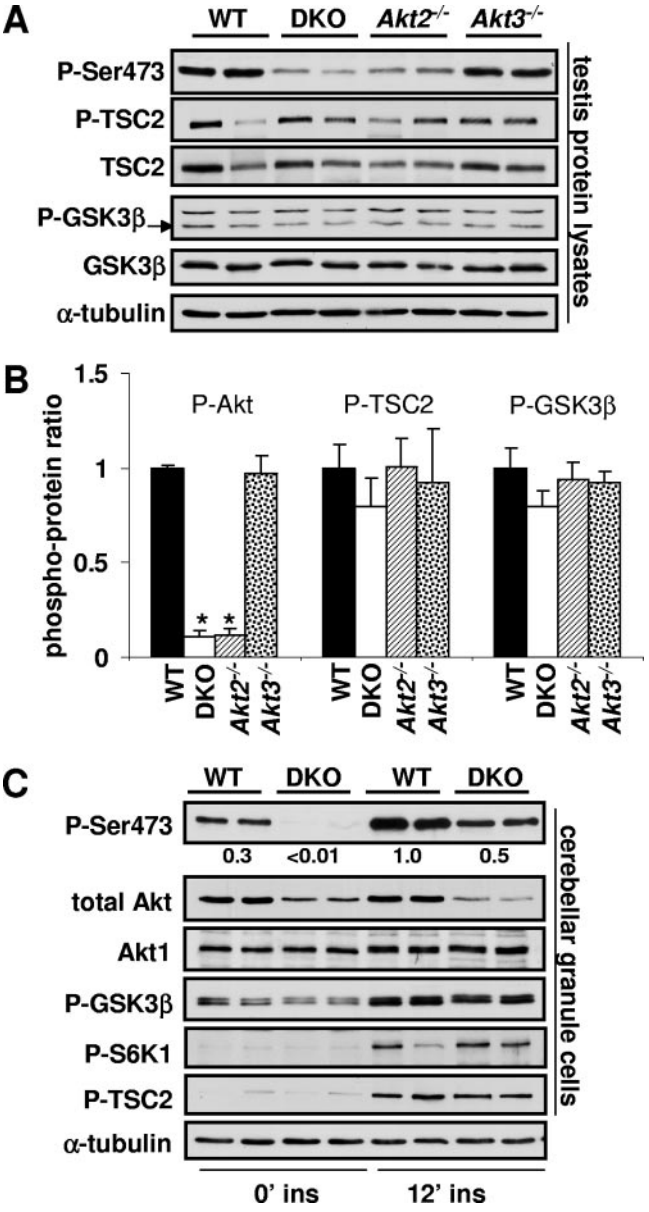

FIG. 4. Phospho-Western blot analysis of downstream targets of Akt. (A) Representative blot showing steady-state phosphorylation of downstream targets of Akt in testes of wild-type (WT), *Akt2*$^{-/-}$, *Akt3*$^{-/-}$, and *Akt2*$^{-/-}$ *Akt3*$^{-/-}$ (DKO) littermate mice. (B) Quantification of phosphorylated Akt and downstream targets. Values are the means for three mice per genotype, error bars depict SEM, and phospho-protein/total protein ratios are relative to the wild-type ratio. Phospho-Akt values were normalized to α-tubulin. (C) Primary cerebellar granule cell cultures of wild-type (WT) and *Akt2*$^{-/-}$ *Akt3*$^{-/-}$ (DKO) mice were serum starved overnight and then stimulated with 100 nM insulin for 12 min. Lysates were analyzed for the phosphorylation status of the indicated downstream targets of Akt. Phospho-Akt bands (P-Ser473) were quantified, and indicated values represent the means for two mice per genotype. Values are relative to stimulated phospho-Akt levels in the wild type and were normalized to the α-tubulin control.

Perturbation of glucose metabolism in *Akt2*$^{-/-}$ *Akt3*$^{-/-}$ mice. The Akt2 isoform of the Akt family has a major role in the regulation of glucose metabolism (36). It is the predominant isoform expressed in insulin-responsive tissues and is in-

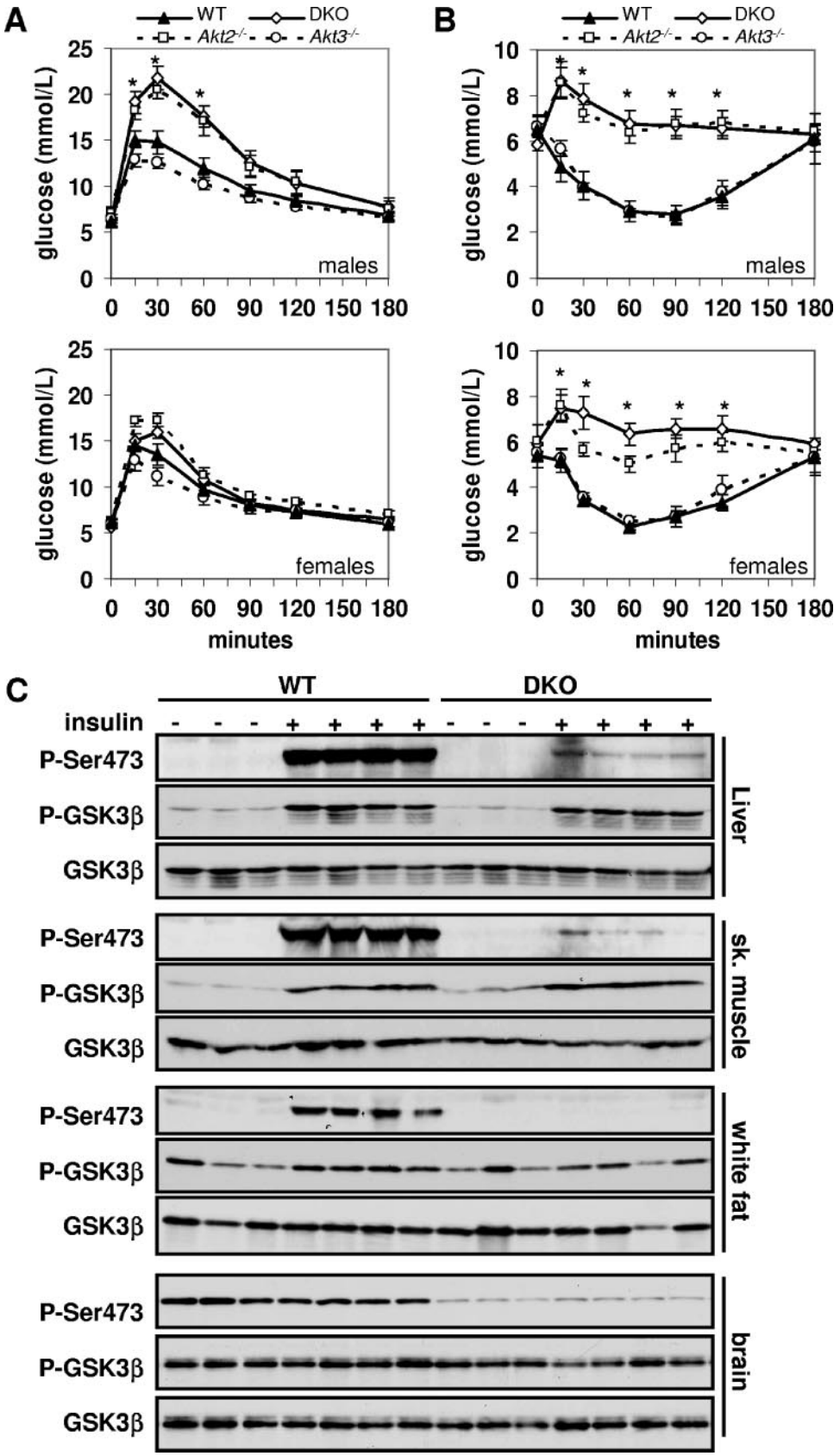

FIG. 5. Glucose metabolism in *Akt2*$^{-/-}$ *Akt3*$^{-/-}$ mice. (A) A glucose tolerance test was performed on 12-week-old male (upper panel) and female (lower panel) mice of the indicated genotypes. The graph depicts arithmetic means ± SEM (n = 8 to 12 for each group) of plasma glucose

volved in the regulation of insulin-stimulated glucose transport, lipogenesis, and glycogen synthesis (1, 7, 15). To investigate glucose metabolism in *Akt2*$^{-/-}$ *Akt3*$^{-/-}$ mice, glucose tolerance and insulin tolerance tests were performed on 3-month-old mice obtained from doubly heterozygous intercrosses (Fig. 5A and B). For the glucose tolerance test, glucose (2 mg/g of body weight) was administered orally to fasted *Akt2*$^{-/-}$ *Akt3*$^{-/-}$, *Akt2*$^{-/-}$, *Akt3*$^{-/-}$, and wild-type littermate mice. For all four genotypes, blood glucose levels peaked 15 to 30 min after glucose administration and returned to baseline after 3 h. *Akt3*$^{-/-}$ mice had similar glucose excursions as wild-type mice. However, in male *Akt2*$^{-/-}$ *Akt3*$^{-/-}$ mice, blood glucose levels rose faster, and at 30 min they were ~50% higher than those of wild-type mice (21.8 ± 1.3 mM versus 14.8 ± 1.2 mM; $P < 0.01$) (Fig. 5A). *Akt2*$^{-/-}$ mice had similar blood glucose levels as *Akt2*$^{-/-}$ *Akt3*$^{-/-}$ mice at all time points. The susceptibility to glucose intolerance was gender dependent because in female mice of all four genotypes, blood glucose levels were not statistically different ($P < 0.05$). Generally, female mice manifest better glucose tolerance than do male mice (16). For assessment of insulin sensitivity, insulin (1 mU/g of body weight) was administered by intraperitoneal injection to fasted *Akt2*$^{-/-}$ *Akt3*$^{-/-}$, *Akt2*$^{-/-}$, *Akt3*$^{-/-}$, and wild-type littermate mice. In wild-type and *Akt3*$^{-/-}$ mice, insulin elicited a >50% decrease in blood glucose levels 60 to 90 min after administration. After 90 min, glucose levels began to recover and reached baseline values 3 h after insulin administration. In contrast, blood glucose levels remained close to baseline levels at all measured time points in *Akt2*$^{-/-}$ *Akt3*$^{-/-}$ and *Akt2*$^{-/-}$ mice. The reduced insulin sensitivity was evident in both male and female mice of the *Akt2*$^{-/-}$ *Akt3*$^{-/-}$ and *Akt2*$^{-/-}$ genotypes.

To further explore the observed differences in glucose disposal, fasting and fed blood glucose and plasma insulin levels were examined in 3-month-old male *Akt2*$^{-/-}$ *Akt3*$^{-/-}$, *Akt2*$^{-/-}$, and wild-type littermate mice. Plasma insulin levels were significantly higher in *Akt2*$^{-/-}$ *Akt3*$^{-/-}$ mice than in the wild type, under both random feeding (4.6- ± 1.6-fold; $P < 0.05$) and fasting (1.9- ± 0.3-fold; $P < 0.05$) conditions (see Table S3 in the supplemental material). In addition, hyperglycemia was observed in *Akt2*$^{-/-}$ *Akt3*$^{-/-}$ mice under random feeding conditions (1.7-fold ± 0.2-fold increase; $P < 0.05$), whereas fasting blood glucose levels were not significantly different from the wild-type levels. We also assessed the percentage of nonenzymatically glycated hemoglobin (hemoglobin A1c [HbA1c]) in male mice of all four genotypes. This value provides an integrated measure of blood glucose levels during a period of approximately 1 month prior to sample removal. Despite the defects in glucose homeostasis, HbA1c levels were similar in both *Akt2*$^{-/-}$ and *Akt2*$^{-/-}$ *Akt3*$^{-/-}$ mice to those in wild-type mice (see Table S3 in the supplemental material). Next, we performed in vivo insulin stimulation in these mice to investigate the induction of Akt phosphorylation in insulin-responsive tissues. Wild-type and *Akt2*$^{-/-}$ *Akt3*$^{-/-}$ mice were made to fast overnight and then injected with a bolus of insulin (10 mU/g) or a saline control. Twelve minutes after injection, insulin-responsive tissues (liver, skeletal muscle, and white fat tissue) were collected. In wild-type mice, Akt became strongly phosphorylated upon insulin stimulation in all three tissues (Fig. 5C). In *Akt2*$^{-/-}$ *Akt3*$^{-/-}$ mice, inducible Akt could also be detected, but phospho-Akt levels were ~10- to 20-fold lower than those in wild-type mice (see Fig. S4 in the supplemental material for quantitation). As a readout for Akt1 activity in *Akt2*$^{-/-}$ *Akt3*$^{-/-}$ mice, we assessed phospho-GSK3β levels in insulin-responsive tissues. Phosphorylation of GSK3β was induced robustly in the liver and skeletal muscle following insulin stimulation, and phosphorylation levels were similar in both *Akt2*$^{-/-}$ *Akt3*$^{-/-}$ and wild-type mice. There was no apparent induction of phospho-GSK3β in white fat in our experimental settings. Peripherally injected insulin was recently shown to also induce Akt phosphorylation in the brain, suggesting an in vivo regulation of the Akt signaling pathway in mouse brain in response to changes in glucose metabolism (29). However, within 12 min of intravenous insulin injection, we could not detect any induction of phospho-Akt in the brain (Fig. 5C), although phospho-Akt levels were consistently lower in *Akt2*$^{-/-}$ *Akt3*$^{-/-}$ mice than in wild-type mice.

DISCUSSION

In order to fully evaluate the impact of the Akt kinase pathway on physiological processes, combined ablation of its isoforms is necessary. Complete inhibition of Akt activity appears to be incompatible with cell survival, but we were able to generate viable Akt mutant mice that contain only a single Akt isoform. Our results provide strong genetic evidence that the Akt1 isoform of the Akt family is sufficient to perform all essential Akt functions in embryonic development and postnatal survival. We observed that *Akt2*$^{-/-}$ *Akt3*$^{-/-}$ mice and even *Akt1*$^{+/-}$ *Akt2*$^{-/-}$ *Akt3*$^{-/-}$ mice, which retain only one functional allele of *Akt1* and have total Akt levels that are up to 10-fold lower than those in wild-type mice, can develop normally and survive with minimal dysfunctions. This is in sharp contrast to the lethal phenotype of mice that contain only Akt3 (*Akt1*$^{-/-}$ *Akt2*$^{-/-}$ mice) or Akt2 (*Akt1*$^{-/-}$ *Akt3*$^{-/-}$ mice) (25, 37). These mice have multiple developmental defects that culminate in lethality at embryonic stage E12 (*Akt1*$^{-/-}$ *Akt3*$^{-/-}$ mice) or the neonatal stage (*Akt1*$^{-/-}$ *Akt2*$^{-/-}$ mice).

concentrations following per os glucose administration (2 g/kg body weight). (B) An insulin tolerance test was performed on 15-week-old male (upper panel) and female (lower panel) mice of the indicated genotypes. The graph depicts arithmetic means ± SEM ($n = 8$ to 10 each group) of plasma glucose concentrations following intraperitoneal injection of insulin (1 mU/g body weight). All genotypes were littermate offspring of *Akt2*$^{+/-}$ *Akt3*$^{+/-}$ matings. Significantly different values obtained for *Akt2*$^{-/-}$ *Akt3*$^{-/-}$ mice (DKO) versus wild-type mice (WT), as determined by one-way ANOVA, are indicated (*, $P < 0.05$). In all four graphs, differences in *Akt2*$^{-/-}$ *Akt3*$^{-/-}$ versus *Akt2*$^{-/-}$ mice were not significant. (C) Active Akt and GSK3β in insulin-responsive tissues of wild-type and *Akt2*$^{-/-}$ *Akt3*$^{-/-}$ mice after in vivo insulin stimulation. Three-month-old male mice were made to fast overnight and injected with either saline (−) or insulin (10 mU/g body weight). After 12 min, the indicated tissues were harvested. Lysates were immunoblotted with the indicated antibodies. Samples are from individual mice ($n = 3$ for saline controls; $n = 4$ for insulin stimulation).

Significantly, combined deficiency of Akt2 and Akt3 affects the determination of whole animal size and individual organ sizes, indicating that Akt1 is not able to fully compensate for the lack of the other isoforms in growth signaling. Akt is a crucial downstream effector of IGF-1 signaling (2, 21). Consistent with a function in cell growth and proliferation, various reports have shown that the expression of activated Akt in specific mouse organs increases organ size (18, 30, 34), whereas ablation of Akt can cause reductions in whole animal growth and/or specific organ sizes (6, 8, 13, 15, 33). In *Akt2*$^{-/-}$ *Akt3*$^{-/-}$ mice, we observed a substantial reduction (25% in males) in body weights compared to those of wild-type mice. Interestingly, no growth deficiencies have been observed in either Akt2 or Akt3 single-knockout phenotypes for the same strain background. However, a mild growth deficiency was shown for *Akt2*$^{-/-}$ mice with a pure DBA/1lacj background (16%) (15). In addition, Akt2 and Akt3 appear to be involved in the regulation of brain and testis size, as the weights of both organs were severely reduced in *Akt2*$^{-/-}$ *Akt3*$^{-/-}$ mice. A testicular phenotype has also been described for *Akt1*$^{-/-}$ mice, which exhibit several morphological abnormalities in the testis (6). In contrast, we found no morphological abnormalities in testes of *Akt2*$^{-/-}$ *Akt3*$^{-/-}$ mice but observed a severe reduction in serum testosterone levels. Interestingly, relative to body weight, brain size was not further reduced in *Akt2*$^{-/-}$ *Akt3*$^{-/-}$ mice compared to Akt3-deficient mice, despite a high expression of Akt2 in the brain (25% of total Akt [13]) which is abrogated in *Akt2*$^{-/-}$ *Akt3*$^{-/-}$ mice. This argues for a selective influence of Akt3 on the regulation of brain size, rather than the size being a result of the total Akt dose in the tissue. Furthermore, Akt3 appears not to contribute to glucose homeostasis in mice, as a combined disruption of Akt2 and Akt3 did not noticeably exacerbate the glucose and insulin intolerance observed in *Akt2*$^{-/-}$ mice.

Detection of active Akt by a phospho-Ser473 antibody showed substantially reduced levels of total active Akt in various tissues of *Akt2*$^{-/-}$ *Akt3*$^{-/-}$ mice both at the steady state and when induced. Surprisingly, phosphorylation levels of critical downstream targets, such as GSK3, TSC2, and S6K, were similar in the *Akt2*$^{-/-}$ *Akt3*$^{-/-}$ mice to those in wild-type controls. Very low levels of active Akt1, the residual isoform, appear to be sufficient to phosphorylate certain downstream targets. However, we cannot formally exclude that these targets may be phosphorylated by another compensatory mechanism. For instance, S6K and p90 ribosomal S6 kinases (RSK) are two other insulin-stimulated protein kinases that can catalyze the phosphorylation of GSK3 in vitro (10, 31, 32). Although Akt appears to be the major kinase phosphorylating GSK3 in vivo upon insulin stimulation (4, 11), S6K and/or RSK may constitute a compensatory mechanism by which GSK3 becomes phosphorylated in Akt-deficient mice.

In conclusion, we provide genetic evidence for a dominant role of Akt1 in embryonic development and postnatal survival. We show that minimal amounts of Akt1 appear to be sufficient for full activation of many downstream targets. In addition, we identify redundant and nonredundant functions of the Akt2 and Akt3 isoforms in growth and glucose metabolism and provide insights into Akt isoform hierarchy.

ACKNOWLEDGMENTS

We thank J. F. Spetz and P. Kopp for their assistance with ES cell culture and embryonic aggregation and R. Portmann for help with Western blot quantifications.

B.D. is supported by the Swiss Cancer League (KFS 1167-09-2001 and KFS 01002-02-2000), O.T. is supported by the Novartis Stiftung für Medizinisch-Biologische Forschung, and Z.Z.Y. is supported, in part, by a grant from Bundesamt für Bildung und Wissenschaft (BBW 98.0176). The Friedrich Miescher Institute for Biomedical Research is funded by the Novartis Research Foundation.

REFERENCES

1. **Bae, S. S., H. Cho, J. Mu, and M. J. Birnbaum.** 2003. Isoform-specific regulation of insulin-dependent glucose uptake by Akt/protein kinase B. J. Biol. Chem. **278:**49530–49536.
2. **Baker, J., J. P. Liu, E. J. Robertson, and A. Efstratiadis.** 1993. Role of insulin-like growth factors in embryonic and postnatal growth. Cell **75:**73–82.
3. **Brazil, D. P., Z. Z. Yang, and B. A. Hemmings.** 2004. Advances in protein kinase B signalling: AKTion on multiple fronts. Trends Biochem. Sci. **29:** 233–242.
4. **Chang, P. Y., Y. Le Marchand-Brustel, L. A. Cheatham, and D. E. Moller.** 1995. Insulin stimulation of mitogen-activated protein kinase, p90rsk, and p70 S6 kinase in skeletal muscle of normal and insulin-resistant mice. Implications for the regulation of glycogen synthase. J. Biol. Chem. **270:**29928–29935.
5. **Cheatham, B., C. J. Vlahos, L. Cheatham, L. Wang, J. Blenis, and C. R. Kahn.** 1994. Phosphatidylinositol 3-kinase activation is required for insulin stimulation of pp70 S6 kinase, DNA synthesis, and glucose transporter translocation. Mol. Cell. Biol. **14:**4902–4911.
6. **Chen, W. S., P. Z. Xu, K. Gottlob, M. L. Chen, K. Sokol, T. Shiyanova, I. Roninson, W. Weng, R. Suzuki, K. Tobe, T. Kadowaki, and N. Hay.** 2001. Growth retardation and increased apoptosis in mice with homozygous disruption of the Akt1 gene. Genes Dev. **15:**2203–2208.
7. **Cho, H., J. Mu, J. K. Kim, J. L. Thorvaldsen, Q. Chu, E. B. Crenshaw III, K. H. Kaestner, M. S. Bartolomei, G. I. Shulman, and M. J. Birnbaum.** 2001. Insulin resistance and a diabetes mellitus-like syndrome in mice lacking the protein kinase Akt2 (PKB beta). Science **292:**1728–1731.
8. **Cho, H., J. L. Thorvaldsen, Q. Chu, F. Feng, and M. J. Birnbaum.** 2001. Akt1/PKBalpha is required for normal growth but dispensable for maintenance of glucose homeostasis in mice. J. Biol. Chem. **276:**38349–38352.
9. **Chung, J., T. C. Grammer, K. P. Lemon, A. Kazlauskas, and J. Blenis.** 1994. PDGF- and insulin-dependent pp70S6k activation mediated by phosphatidylinositol-3-OH kinase. Nature **370:**71–75.
10. **Cross, D. A. E., D. R. Alessi, P. Cohen, M. Andjelkovich, and B. A. Hemmings.** 1995. Inhibition of glycogen synthase kinase-3 by insulin mediated by protein kinase B. Nature **378:**785–789.
11. **Cross, D. A. E., P. W. Watt, M. Shaw, J. van der Kaay, C. P. Downes, J. C. Holder, and P. Cohen.** 1997. Insulin activates protein kinase B, inhibits glycogen synthase kinase-3 and activates glycogen synthase by rapamycin-insensitive pathways in skeletal muscle and adipose tissue. FEBS Lett. **406:** 211–215.
12. **Dudek, H., S. R. Datta, T. F. Franke, M. J. Birnbaum, R. Yao, G. M. Cooper, R. A. Segal, D. R. Kaplan, and M. E. Greenberg.** 1997. Regulation of neuronal survival by the serine-threonine protein kinase Akt. Science **275:** 661–665.
13. **Easton, R. M., H. Cho, K. Roovers, D. W. Shineman, M. Mizrahi, M. S. Forman, V. M. Lee, M. Szabolcs, R. de Jong, T. Oltersdorf, T. Ludwig, A. Efstratiadis, and M. J. Birnbaum.** 2005. Role for Akt3/protein kinase Bgamma in attainment of normal brain size. Mol. Cell. Biol. **25:**1869–1878.
14. **Fingar, D. C., S. Salama, C. Tsou, E. Harlow, and J. Blenis.** 2002. Mammalian cell size is controlled by mTOR and its downstream targets S6K1 and 4EBP1/eIF4E. Genes Dev. **16:**1472–1487.
15. **Garofalo, R. S., S. J. Orena, K. Rafidi, A. J. Torchia, J. L. Stock, A. L. Hildebrandt, T. Coskran, S. C. Black, D. J. Brees, J. R. Wicks, J. D. McNeish, and K. G. Coleman.** 2003. Severe diabetes, age-dependent loss of adipose tissue, and mild growth deficiency in mice lacking Akt2/PKB beta. J. Clin. Investig. **112:**197–208.
16. **Goren, H. J., R. N. Kulkarni, and C. R. Kahn.** 2004. Glucose homeostasis and tissue transcript content of insulin signaling intermediates in four inbred strains of mice: C57BL/6, C57BLKS/6, DBA/2, and 129X1. Endocrinology **145:**3307–3323.
17. **Inoki, K., Y. Li, T. Zhu, J. Wu, and K. L. Guan.** 2002. TSC2 is phosphorylated and inhibited by Akt and suppresses mTOR signalling. Nat. Cell Biol. **4:**648–657.
18. **Kim, Y. K., S. J. Kim, A. Yatani, Y. Huang, G. Castelli, D. E. Vatner, J. Liu, Q. Zhang, G. Diaz, R. Zieba, J. Thaisz, A. Drusco, C. Croce, J. Sadoshima, G. Condorelli, and S. F. Vatner.** 2003. Mechanism of enhanced cardiac function in mice with hypertrophy induced by overexpressed Akt. J. Biol. Chem. **278:**47622–47628.
19. **Kwiatkowski, D. J., H. Zhang, J. L. Bandura, K. M. Heiberger, M. Glogauer,**

N. el-Hashemite, and H. Onda. 2002. A mouse model of TSC1 reveals sex-dependent lethality from liver hemangiomas, and up-regulation of p70S6 kinase activity in Tsc1 null cells. Hum. Mol. Genet. **11:**525–534.
20. **Lawlor, M. A., and D. R. Alessi.** 2001. PKB/Akt: a key mediator of cell proliferation, survival and insulin responses? J. Cell Sci. **114:**2903–2910.
21. **Liu, J. P., J. Baker, A. S. Perkins, E. J. Robertson, and A. Efstratiadis.** 1993. Mice carrying null mutations of the genes encoding insulin-like growth factor I (Igf-1) and type 1 IGF receptor (Igf1r). Cell **75:**59–72.
22. **Manning, B. D., and L. C. Cantley.** 2003. Rheb fills a GAP between TSC and TOR. Trends Biochem. Sci. **28:**573–576.
23. **Manning, B. D., A. R. Tee, M. N. Logsdon, J. Blenis, and L. C. Cantley.** 2002. Identification of the tuberous sclerosis complex-2 tumor suppressor gene product tuberin as a target of the phosphoinositide 3-kinase/Akt pathway. Mol. Cell **10:**151–162.
24. **Manning, G., G. D. Plowman, T. Hunter, and S. Sudarsanam.** 2002. Evolution of protein kinase signaling from yeast to man. Trends Biochem. Sci. **27:**514–520.
25. **Peng, X. D., P. Z. Xu, M. L. Chen, A. Hahn-Windgassen, J. Skeen, J. Jacobs, D. Sundararajan, W. S. Chen, S. E. Crawford, K. G. Coleman, and N. Hay.** 2003. Dwarfism, impaired skin development, skeletal muscle atrophy, delayed bone development, and impeded adipogenesis in mice lacking Akt1 and Akt2. Genes Dev. **17:**1352–1365.
26. **Potter, C. J., L. G. Pedraza, and T. Xu.** 2002. Akt regulates growth by directly phosphorylating Tsc2. Nat. Cell Biol. **4:**658–665.
27. **Scheid, M. P., and J. R. Woodgett.** 2001. PKB/AKT: functional insights from genetic models. Nat. Rev. Mol. Cell. Biol. **2:**760–768.
28. **Schubert, M., D. P. Brazil, D. J. Burks, J. A. Kushner, J. Ye, C. L. Flint, J. Farhang-Fallah, P. Dikkes, X. M. Warot, C. Rio, G. Corfas, and M. F. White.** 2003. Insulin receptor substrate-2 deficiency impairs brain growth and promotes tau phosphorylation. J. Neurosci. **23:**7084–7092.
29. **Schubert, M., D. Gautam, D. Surjo, K. Ueki, S. Baudler, D. Schubert, T. Kondo, J. Alber, N. Galldiks, E. Kustermann, S. Arndt, A. H. Jacobs, W. Krone, C. R. Kahn, and J. C. Bruning.** 2004. Role for neuronal insulin resistance in neurodegenerative diseases. Proc. Natl. Acad. Sci. USA **101:**3100–3105.
30. **Shioi, T., J. R. McMullen, P. M. Kang, P. S. Douglas, T. Obata, T. F. Franke, L. C. Cantley, and S. Izumo.** 2002. Akt/protein kinase B promotes organ growth in transgenic mice. Mol. Cell. Biol. **22:**2799–2809.
31. **Sutherland, C., and P. Cohen.** 1994. The alpha-isoform of glycogen synthase kinase-3 from rabbit skeletal muscle is inactivated by p70 S6 kinase or MAP kinase-activated protein kinase-1 in vitro. FEBS Lett. **338:**37–42.
32. **Sutherland, C., I. A. Leighton, and P. Cohen.** 1993. Inactivation of glycogen synthase kinase-3 beta by phosphorylation: new kinase connections in insulin and growth-factor signalling. Biochem. J. **296:**15–19.
33. **Tschopp, O., Z. Z. Yang, D. Brodbeck, B. A. Dummler, M. Hemmings-Mieszczak, T. Watanabe, T. Michaelis, J. Frahm, and B. A. Hemmings.** 2005. Essential role of protein kinase B gamma (PKB gamma/Akt3) in postnatal brain development but not in glucose homeostasis. Development **132:**2943–2954.
34. **Tuttle, R. L., N. S. Gill, W. Pugh, J. P. Lee, B. Koeberlein, E. E. Furth, K. S. Polonsky, A. Naji, and M. J. Birnbaum.** 2001. Regulation of pancreatic beta-cell growth and survival by the serine/threonine protein kinase Akt1/PKBalpha. Nat. Med. **7:**1133–1137.
35. **van Slegtenhorst, M., M. Nellist, B. Nagelkerken, J. Cheadle, R. Snell, A. van den Ouweland, A. Reuser, J. Sampson, D. Halley, and P. van der Sluijs.** 1998. Interaction between hamartin and tuberin, the TSC1 and TSC2 gene products. Hum. Mol. Genet. **7:**1053–1057.
36. **Whiteman, E. L., H. Cho, and M. J. Birnbaum.** 2002. Role of Akt/protein kinase B in metabolism. Trends Endocrinol. Metab. **13:**444–451.
37. **Yang, Z. Z., O. Tschopp, N. Di-Poi, E. Bruder, A. Baudry, B. Dummler, W. Wahli, and B. A. Hemmings.** 2005. Dosage-dependent effects of Akt1/protein kinase Balpha (PKBalpha) and Akt3/PKBgamma on thymus, skin, and cardiovascular and nervous system development in mice. Mol. Cell. Biol. **25:**10407–10418.
38. **Yang, Z. Z., O. Tschopp, M. Hemmings-Mieszczak, J. Feng, D. Brodbeck, E. Perentes, and B. A. Hemmings.** 2003. Protein kinase B alpha/Akt1 regulates placental development and fetal growth. J. Biol. Chem. **278:**32124–32131.